Research Paper

Inclusive Mobility in High-Density Cities: Understanding Elderly metro travel through Smart Card Data and XAI

Bo Lu, College of Architecture & Urban Planning, Hunan City University, China

Sijun Guo, College of Architecture & Urban Planning, Hunan City University, China

Yizhe Huang, College of Architecture & Urban Planning, Hunan City University, China

Abstract

This research examines the influence of built environment metrics on elderly metro travel in Shanghai by leveraging 1.3 million Smart Card records and Explainable Artificial Intelligence(XAI). Employing a Geographically Weighted Random Forest model with SHAP interpretability, the study exposes the nonlinear and spatially heterogeneous dynamics between urban forms and age-related mobility. Key findings indicate that functional amenities,specifically shopping, living services, and governmental facilities,are the most significant predictors of travel patterns. In contrast, density indicators like floor area ratio and intersection density exhibit less influence than anticipated, largely due to saturation effects in highly urbanized areas. Crucially, the analysis reveals optimal BE thresholds, suggesting that while moderate density fosters accessibility, excessive urban complexity may hinder elderly mobility. Furthermore, station clustering identifies three spatial typologies that substantiate localized built environment effects. By bridging AI interpretability with spatial modeling, this work offers actionable insights for creating inclusive, equitable, and resilient transport systems, supporting a transition toward responsive and age-friendly urban governance.

Keywords

Older adults' mobility, built environment, Explainable Artificial Intelligence (XAI), high density , nonlinear effects, inclusive

1. Introduction

The rapid acceleration of global population aging, with the WHO predicting 2.1 billion people over 60 by 2050, presents profound challenges for urban spatial equity (WHO, 2024). In high-density metropolises like Shanghai, the metro system is a cornerstone of "24-hour city" mobility, providing affordable access to healthcare, social participation, and daily services (Diao et al., 2024). To foster inclusive mobility, Shanghai implemented the "Baotong Card" policy, offering free public transit to seniors over 70, thereby generating massive Smart Card Data (SCD) that reflects the actual travel demands of the elderly (Government, 2017).

While the "5D" built environment (BE) framework, comprising density, diversity, design, destination accessibility, and distance to transit, has been widely used to analyze travel behavior (Ewing and Cervero, 2010), its application to elderly metro mobility in hyper-dense contexts remains limited. Existing studies often prioritize commuting patterns or pedestrian friendliness, frequently relying on linear models that overlook the complex, non-linear interactions between BE and mobility. Specifically, high-density environments may foster accessibility yet simultaneously introduce spatial complexity and overcrowding that discourage elderly travel (Yang et al., 2024a). Furthermore, traditional surveys fail to capture continuous travel chains, leaving a gap in understanding how specific BE attributes produce threshold dynamics or spatially heterogeneous impacts.

The digital transformation of urban planning, particularly through Explainable Artificial Intelligence (XAI), offers an unprecedented opportunity to transcend static analysis. By leveraging SCD and machine learning, we can now model large-scale mobility patterns while elucidating the underlying mechanisms of specific spatial factors.

Against this background, this study utilizes Shanghai as a case to investigate elderly metro travel patterns. We address three critical questions: (1) How can SCD effectively identify elderly travel chains in dense urban environments? (2) Which BE indicators most significantly influence destination selection? and (3) To what extent do these influences exhibit nonlinear thresholds or spatial heterogeneity? By addressing these, this research advances both methodological modeling and evidence-based planning for inclusive, age-friendly urban environments.

The remainder of this paper is structured as follows: Section 2 outlines the methodology and datasets; Section 3 presents the findings and policy implications; and Section 4 provides conclusions.

2. Methodology

2.1. Study area and data

Shanghai, a hyper-dense megacity with the world's largest metro system, serves as the study area (Figure 1). By 2024, residents aged 70+ accounted for nearly 20% of its population (Affairs, 2025), making it a critical case for elderly mobility research.

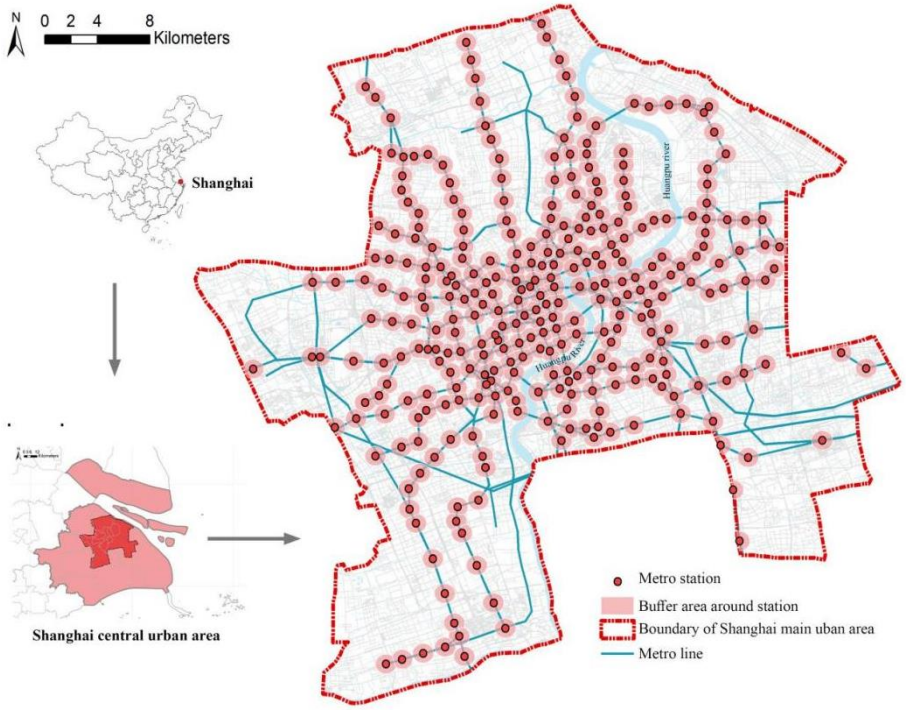

Figure 1.Study area. Source: Author.

We utilized 1.3 million anonymized smart card records (Jan 2023 – Aug 2024) from the "Baotong Card" system. To ensure data reliability, we excluded: (1) incomplete records or trips <5 or >120 minutes; and (2) extreme users (infrequent users with <10 trips or excessive users with >2,000 trips). The final dataset comprises 1,297,400 trips from 3,487 eligible users.

Following the "5D" framework, 20 BE indicators were constructed from 2023–2024 spatial datasets (See Table 1). Based on previous studies (Liu et al., 2025b), we measured these indicators within 800m station catchments using Voronoi polygons to prevent overlapping. To address elderly needs, POI data were reclassified into residential, commercial, recreational, medical, and governmental functions.

Table 1.Descriptive statistics of built environment indicators

Indicators	Initial	Description	Mean	Std	Source
Floor area ratio	FAR	The ratio of the total building floor area to the total area of the buffer area	2.99	1.24	/https://www.resdc.cn/
Road density	RD	The cumulative length of roads within the buffer zone(km) divided by the total area of buffer area	15.20	6.98	https://www.openstreetmap.org/
Intersection density	ID	The cumulative number of intersections within the buffer zone divided by the total area of buffer area	19.58	18.37	https://www.openstreetmap.org/
Land use diversity	LDI	Calculated using the Shannon diversity index($SHDI = -\frac{\sum_1^n P_i \ln P_i}{\ln(n)}$) based on the area proportions of land use(e.g., residential, commercial, and industrial)within the buffer area	0.88	0.37	https://data.sh.gov.cn/ https://www.resdc.cn/
Point of interests diversity	PDI	Calcualted using the Shannon diversity index($SHDI = -\frac{\sum_1^n P_i \ln P_i}{\ln(n)}$) of functional facilities(e.g., living support services,	1.66	0.25	https://www.amap.com

		shopping services) within the buffer area			
Road connectivity	RC	The average node degree in the road network within the buffer area	2.14	0.07	https://www.openstreetmap.org/
Normalized Difference Vegetation Index	NDVI	The average Normalized Difference Vegetation Index value within the buffer area	0.11	0.03	https://earthengine.google.com/
Distance to nearest park	Dist_P	The shortest network distance from metro station to nearest park within the buffer area	732	849	https://www.resdc.cn/
Average distance to the metro station	Dist_M	The shortest street-based network distance from the station centroid to the nearest accessible public green space(m)	846	363	https://service.shmetro.com/
Distance to city center	DIST_C	The calculate euclidean distance from the station to the center of the area(m)	5,457	3,813	https://www.openstreetmap.org/
Government services facilities	POI_Gov	The cumulative number of government services facilities within the buffer area	28	23	https://www.amap.com
Recreational and leisure services facilities	POI_Rec	The cumulative number of recreational and leisure services facilities, such as fishing park, orchard, camping site, sports venue, chess room, within the buffer area	9	9	https://www.amap.com
Medical and healthcare services facilities	POI_Med	The cumulative number of medical and healthcare facilities, such as hospital, healthcare service facility, within the buffer area	9	8	https://www.amap.com
Living services facilities	POI_Liv	The cumulative number of living service facilities, such as fast food shop, bank, post office, laundry house, within the buffer area	28	25	https://www.amap.com
Shopping services facilities	POI_Sho	The cumulative number of shopping service facilities, sucha as mall, market, pet and plant market, within the buffer area	29	24	https://www.amap.com
Cultural and educational facilities	POI_Cul	The cumulative number of cultural service facilities, such as museum, library, art gallery, exhibition hall, within the buffer area	14	15	https://www.amap.com
Route betweenness centrality	BTC	The frequency with which a station serves as a bridge on the shortest topological paths ($\boldsymbol{\beta(v)} = \sum_{s \neq v \neq t} \frac{\sigma(s,t\|v)}{\sigma(s,t)}$).between all other station	0.7	0.6	https://service.shmetro.com/
Number of subway connecting lines	SUB_L	The mean line count per station, serving as a proxy for the transfer potential and structural importance of the transit node	1.33	0.60	https://service.shmetro.com/
Population density of older adults above 70	POP70	The mean population count of residents aged 70 and above residing within the buffer area	6267	3389	https://www.worldpop.org/
House price	HOU_P	The mean value of house price within the buffer area(¥).	75,566	25,067	https://m.anjuke.com/bj/

Shanghai's morphology is characterized by high density and functional intensity (Average FAR = 2.99). High RD and ID support pedestrian circulation, though average NDVI remains low due to compact urban development. Significant spatial heterogeneity exists in Hou_P(Mean = ¥75,566/m²) and elderly population distribution, reflecting substantial socioeconomic variations across metro catchments. Multicollinearity checks confirmed the suitability of all selected factors for model construction.

2.2. Analytical framework

The analytical framework of this study consists of four interrelated phases (Figure 2). Part 1 involves data integration and preprocessing, where 1.3 million “Baotong Card” records are combined with multi-source built environment (BE) data. Following data cleaning and trip-chain reconstruction, we establish a BE variable system and conduct multicollinearity checks to ensure indicator independence. Part 2 focuses on station identification using a center-point algorithm and frequency-dwell-time rules. This process demarcates home station departure (HD) and activity station arrival (AR) volumes, forming the basis for spatiotemporal pattern analysis.

In Part 3, a Geographically Weighted Random Forest (GWRF) model is constructed to quantify the spatially varying relationships between BE indicators and elderly metro ridership within station catchments. We incorporate the SHAP (SHapley Additive exPlanations) method to provide a global interpretation of feature importance and identify non-linear threshold effects. Finally, Part 4 implements spatial clustering and local inference. Using K-means clustering based on aging population density and HD/AR ratios, we classify metro stations into distinct typologies. Local SHAP inference is then applied to representative stations within each cluster to uncover spatial heterogeneity and the specific driving factors influencing the elderly metro experience across different urban contexts.

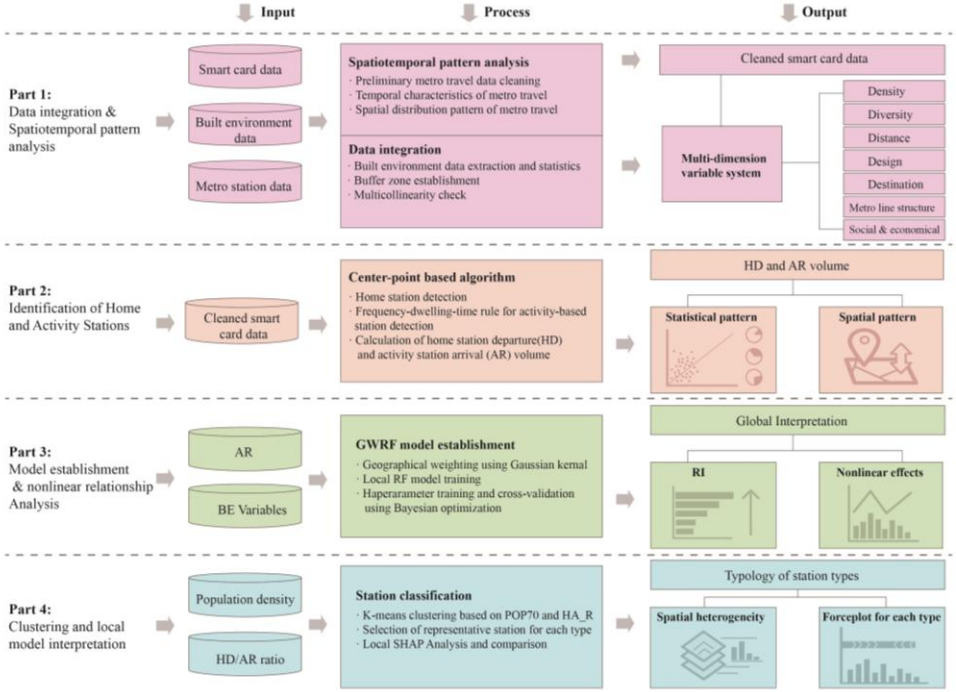

Figure 2.Analytical framework of the study. Source: Author.

2.3 Center-point based algorithm for home and activity stations detection

Following previous studies and considering the behavioral characteristics of older adults (Zou et al., 2018), the center-point based detection algorithm was utilized to detect the home, and activity stations for older adult metro travelers, through the application of the daily record of

travel of users in the metro service. The procedure is subdivided into three parts (Figure 3). First, the first boarding station and the last available station of the day were detected for every user, thereby producing daily home, activity pairs for a closed loop journey.

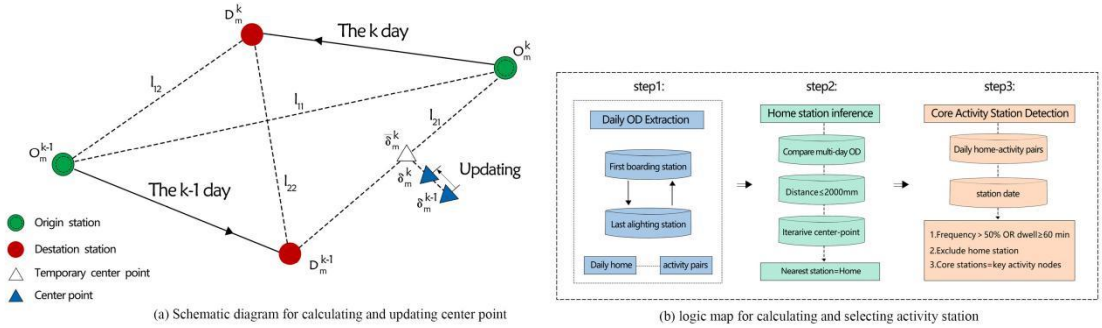

(a) Schematic diagram for calculating and updating center point

(b) logic map for calculating and selecting activity station

Figure 3.Diagram for center-point based algorithm. Source: Author.

Secondly, the first and last stations of the daily records of each user were compared, and the distance between the spatial coordinates was calculated on a day-to-day basis. In the event the daily station coordinates happened to be within a 2000 m threshold, then an iterative process of recalculation of the geometrical midpoint is used so as to compute periodicity in the obtained “center point” for several days. The station nearest to this center-point is allocated to the user as the home station of the user. This arrangement gives the advantage of eliminating random noise resulting from not infrequent periodic trips, with the result that the home station obtained is based upon actual periodicity of travel.

Thirdly, the probable activity stations are summed together according to frequency of visitation, and the duration of dwell. Stations, for which to account for dwell duration, over sixty minutes is spent, and for which more than fifty per cent of the total visits occur, are termed core activity stations.

2.4 GWRF model construction

To quantify the spatially varying and nonlinear influences of BE indicators on elderly metro ridership, we developed a Geographically Weighted Random Forest (GWRF) model. This hybrid approach integrates the nonlinear learning capacity of Random Forest (RF) with the spatial weighting mechanism of Geographically Weighted Regression (Georganos et al., 2021).The modeling involved four key steps: (1) Hyperparameter Optimization: A global RF model was tuned via Bayesian optimization (trees: 200–800; depth: 5–20). (2) Spatial Weighting: We implemented Gaussian distance-decay weighting based on the 50 nearest stations (k = 50), training local RF models for each station to capture spatial heterogeneity. (3) Validation: Five-fold spatial cross-validation yielded an average R^2 of 0.53 and RMSE of 1506, significantly outperforming the baseline RF model. (4) Interpretability: The SHAP algorithm was applied to decompose predictions into additive feature contributions, enabling both global importance ranking and local dependency analysis (Lundberg, 2017).

3. Results and Discussion

3.1. Spatiotemporal pattern of older adults' metro travel

The study examined the metro travels of older adults by employing various time-related levels:hourly, weekly, monthly, trip duration and travel distance range (See Figure 4a-4b). Overall, Elderly metro trips in Shanghai exhibit a stable and rhythmic temporal pattern . Hourly distribution reveals a "bimodal" pattern with peaks at 8:00–10:00 and 15:00–17:00, indicating a clear "off-peak" preference to avoid peak-hour congestion. Weekly stability and seasonal fluctuations, with activity peaks in spring and autumn, suggest that elderly mobility is primarily driven by non-commute demands and is climate-sensitive. Most trips are short-to-medium distance, with durations of 10–30 minutes and distances under 10 km (See Figure 4c-4d).

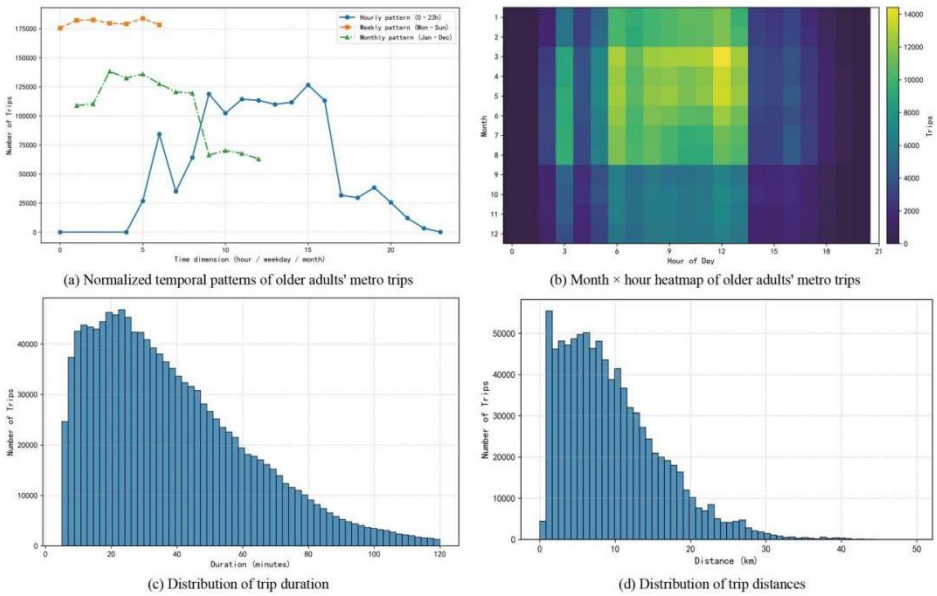

Figure 4.Spatiotemporal distribution and travel distance characteristics of metro usage among older adults. Source: Author.

3.2. Identification of home and activity stations

Following data cleansing and center-point detection, 895,053 valid trips from 3,407 users were analyzed. Both home station departures (HD) and activity station arrivals (AR) exhibit highly right-skewed distributions, indicating significant spatial heterogeneity (Figure 5a-5c). The scatterplot reveals that most stations sit above the 1:1 diagonal, with AR volumes frequently exceeding HD, suggesting that elderly travel is characterized by diverse origins but concentrated destinations, a marked contrast to the balanced flows of regular commuting.

Spatially, a distinct core-periphery differentiation emerges (Figure 5d). High-AR stations are densely clustered within the Inner Ring (Huangpu, Jing'an, and Xuhui), driven by the concentration of multi-functional amenities. Conversely, HD stations are more prevalent in the middle and outer rings, particularly along Lines 1, 7, 9, and 13, which serve major residential

aging communities. This "peripheral living-central activity" framework highlights the functional magnetism of the urban core for seniors and underscores the spatial mismatch between residential concentrations and service-rich activity hubs in newly developed peripheral areas.

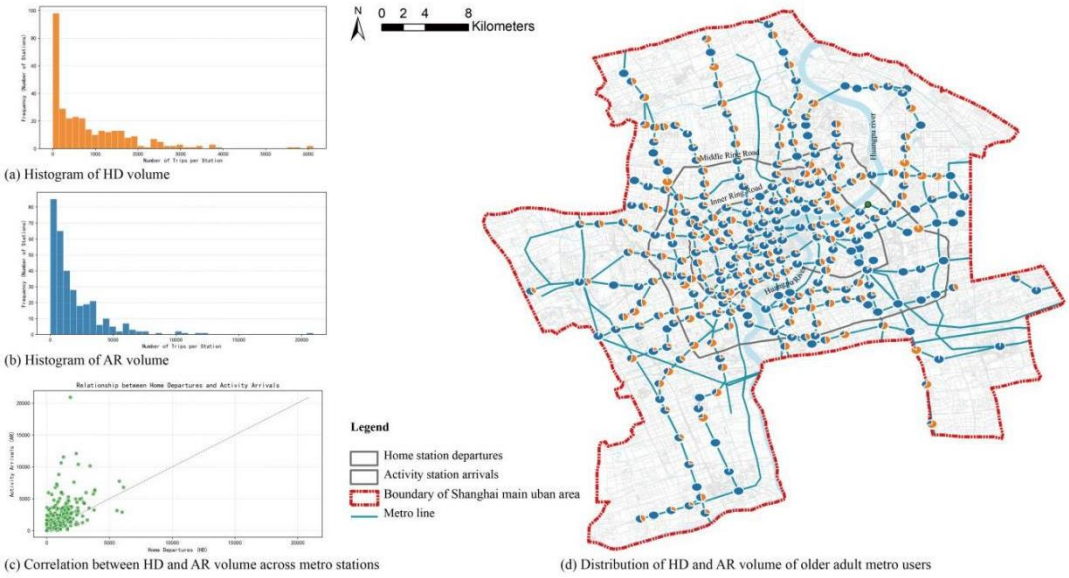

Figure 5.Spatial and statistical identification of HD and AR volume of older adult metro travelers. Source: Author.

3.3. RI and nonlinear effects of built environment indicators

Given that metro travel is inherently purpose-oriented, this study adopts AR volume as the dependent variable to more effectively examine how BE indicators and their threshold effects influence metro travel among older adults. The SHAP feature importance plot (Figure 6a) and summary plot (Figure 6b) indicate that several indicators related to functional intensity and service accessibility play dominant roles in explaining older adults metro destinations.

The diagram reveals that functional intensity and service accessibility are the primary drivers of elderly metro travel. Functional POIs, specifically living services (POI_Liv), shopping (POI_Sho), and governmental facilities (POI_Gov), emerged as the top three predictors, each with mean absolute SHAP values exceeding 0.15. This confirms a strong preference for destinations offering daily convenience and administrative services, aligning with previous studies (Cerin et al., 2017; Zang et al., 2019). Recreational and cultural POIs also show moderate positive contributions, reflecting the rising importance of leisure-oriented mobility.

Furthermore, the concentration of the elderly population (POP70) and metro network connectivity (SUB_L) exhibit high importance, indicating a synergy between demand-side aggregation and supply-side facilitation. Interestingly, traditional density metrics (e.g., FAR, intersection density) and environmental factors (NDVI) play a secondary role. This suggests that in Shanghai’s ultra-dense context, physical density has reached a "saturation point" where its

marginal effect diminishes, whereas the specific functional composition of the built environment provides a more direct and significant influence on elderly destination choices.

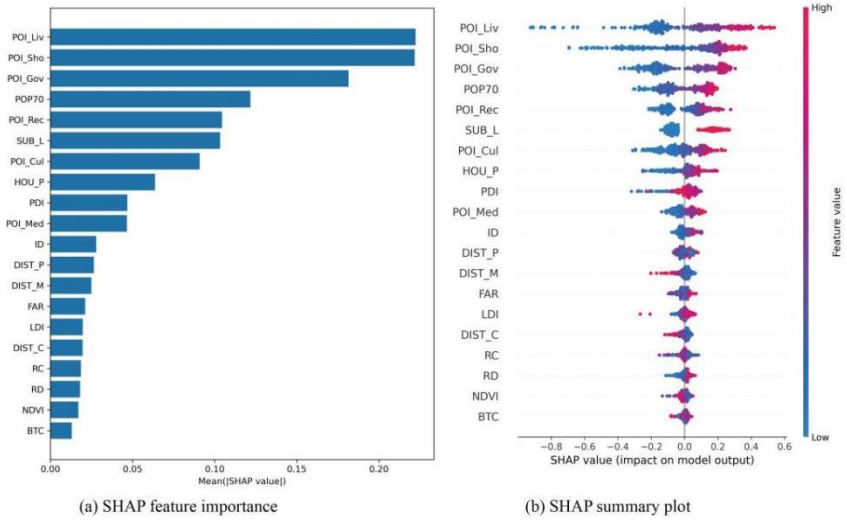

Figure 6. RI ranking and SHAP summary plot. Source: Author.

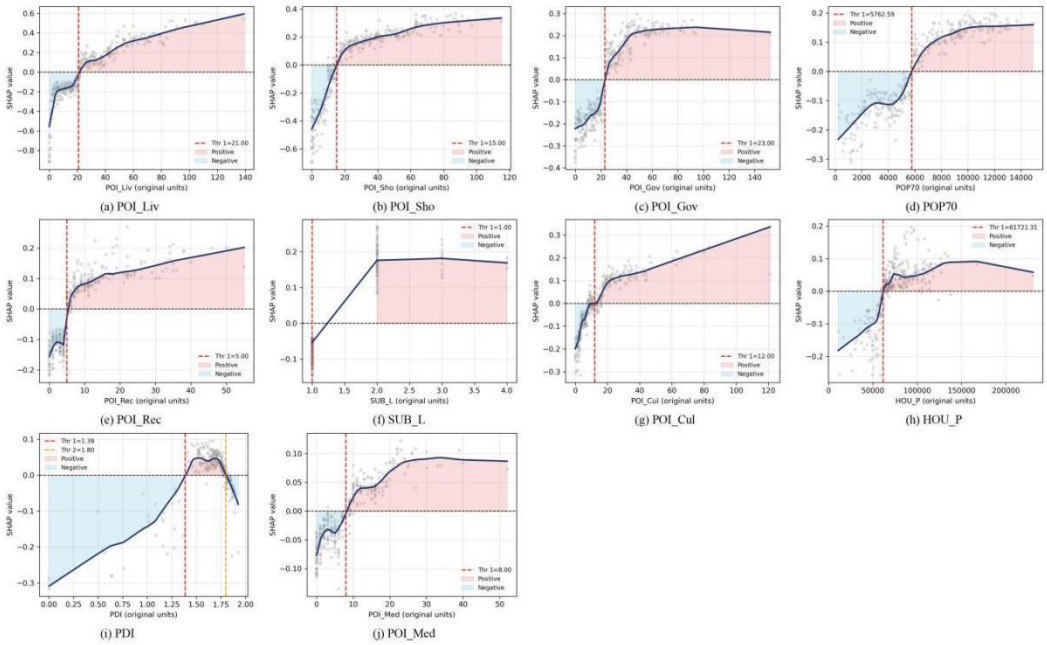

Figure 7. LDP for top 10 built environment indicators. Source: Author

Figure 7 displays the local dependence plots (LDPs) for the 10 BE indicators that matter most in influencing older adults' metro ridership, noting their nonlinear relationships (or threshold effects). Most of the top ten indicators exhibit a monotonic increasing relationship with the SHAP values. In other words, higher levels of these BE indicators are generally correlated to an increasing probability or value of metro trip destination attractiveness to older adults. Each indicator has generally linear thresholds at certain points, beyond which marginal

contributions of the indicator remain stable. However, POI diversity index (PDI) has a clear inverted U-shape pattern exhibiting two significant thresholds at approximately 1.39 and 1.80, indicating that a moderately diverse land-use and POI character may support older adults' metro travel use, likely due to an appropriate blend of opportunities for living, services and recreational activities. Yet, beyond this point of additional functional heterogeneity, destination attractiveness may decline (Guo et al., 2023). The decline beyond its upper thresholds may be explained by the effects of spatial disaggregation or functional competition whereby oversaturation of land uses diminishes functional clarity and convenience for travelers having to navigate residential areas in their daily activities, potentially discouraging older adults from traveling to those places.

While the majority of the indicators indicate a positive, monotonic effect, the marginal gains from increasing levels start to taper once the previously discussed thresholds are met, indicating that saturation effects exist in ultra-dense urban environments, like Shanghai. For example, indicators POI_Liv, POI_Sho and POW_Gov all show some steep increases in SHAP values up to about 20 units of their respective thresholds, after which the influence all plateaus. There is some similarly saturating behavior observed as well with POP70, SUB_L, and HOU_P suggesting that the advantages of spatially-co-located service facilities, high population density, transfer-connectedness or housing price concentrations also reach limits once basic accessibility and intensities of function have been achieved(Guo et al., 2023, Wang et al., 2023, Yang et al., 2024c) .

3.4. Local spatial classification and driving factors analysis

To further exam the spatial heterogeneity of older adults metro usage in relation to different population density, this part categorizes the metro stations and clarifies the local factors affecting them(Yang et al., 2024b, Liu et al., 2025a). The classification was achieved by using the K-means cluster algorithm using two key indicators, the people density of older adults above 70 (POP70) and HD / AR ratio (HA_R). The number of clusters was found to be three (k = 3), with the maximum value of the silhouette index, which is a degree of the cluster validity and spatial separability (Figure 8).

To address spatial heterogeneity, we categorized 285 metro stations into three clusters using K-means based on elderly population density (POP70) and Home-Activity ratio (HA_R) (Figure 8a). SHAP-based local driving factor analysis was then conducted for representative stations in each cluster (Figures 8b–8c).

Type 1: Urban Core Hubs (n=193). Predominantly located within the inner ring, these stations are characterized by high functional density and land-use mix. Using the Shanghai Natural History Museum station as a representative, analysis shows that while administrative (POI_Gov) and cultural functions strongly attract elderly travel, a relative deficiency in daily living services (POI_Liv) can exert negative impacts. This suggests that enhancing "living service" granularity in hyper-dense cores is vital for age-friendliness.

Type 2: Mature Residential Zones (n=56). Distributed along the middle ring, these areas are dominated by residential and educational uses. For the Heshahangcheng station, lower housing prices (HOU_P) act as a positive pull factor for elderly relocation. However, low intersection

density (ID) and a lack of cultural POIs significantly constrain mobility, highlighting a need for improved street permeability and "soft" cultural infrastructure.

Type 3: Developing/Industrial Fringes (n=36). Located in urban peripheries with lower densities. Taking Ziteng Road station as an example, even limited shopping (POI_Sho) and recreational (POI_Rec) facilities provide strong positive stimulation for metro trips, serving as essential social nodes. Conversely, higher greenery (NDVI) often contributes negatively here, as it frequently represents inaccessible industrial green belts rather than functional parks.

In summary, the driving mechanisms of elderly mobility are context-specific: Type 1 requires functional "fine-weaving" of services; Type 2 necessitates structural connectivity and cultural enrichment; and Type 3 relies on the provision of basic commercial anchors to stimulate social participation.

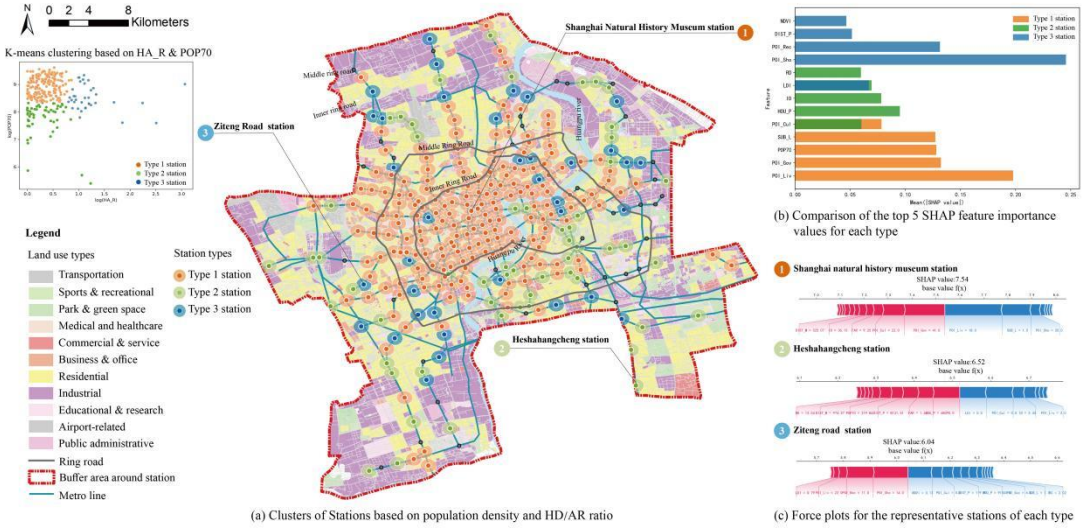

(a) Clusters of Stations based on population density and HD/AR ratio

(b) Comparison of the top 5 SHAP feature importance values for each type

(c) Force plots for the representative stations of each type

Figure 8. Classification and local explanation for older adults' metro travel patterns. Source: Author.

3.5. Policy implication

The metro travel behavior of older adults is significantly moderated by their surroundings, including urban living services, environmental quality, and accessibility networks. Our nonlinear analysis confirms that in high-density settings, the "more is better" principle does not always hold for density-related indicators. Consequently, this research suggests transitioning from traditional TOD frameworks toward human-centric, functionally adaptive, and systemically integrated paradigms. Rather than focusing solely on density, planning should prioritize the alignment of spatial infrastructure with the everyday patterns and sensory experiences of older adults. Leveraging digital tools for real-time mobility monitoring can facilitate a shift toward adaptive, behavior-informed governance.

Focused planning must also account for spatial variations. In core downtown areas (Type 1), high built-up density and complex interchanges often cause cognitive load and psychological anxiety for seniors. Urban redevelopment should therefore prioritize spatial legibility and green

resting spaces. Moreover, as gentrification often displaces small-scale services, TOD initiatives must reintegrate daily-life functional amenities that support social participation.

In outer-center residential areas and newly developed sub-centres (Type 2), which hold significant growth potential for elderly ridership, efforts should strengthen non-commuter anchors such as healthcare, cultural, and leisure amenities. Creating “15-minute neighbourhoods” and improving streetscape safety and connectivity are essential to providing mentally accommodating environments in these zones.

Finally, in newly developing peripheral or transforming industrial areas (Type 3), emphasis should be placed on introducing diverse retail and aging-responsive infrastructure to nurture inclusive neighbourhoods. Improving the connectivity and recreational programming of available green spaces can further encourage outdoor activity. To foster equitable mobility, it is imperative to enhance cross-district transit connectivity and deploy universal pedestrian networks to bridge the last-mile gap.

4. Conclusion

This study examines inclusive mobility in high-density areas by analyzing older adults’ metro travel behavior through 1.3 million smart card records and the GWRF-SHAP framework. Our findings reveal that functional amenities drive elderly mobility through complex, nonlinear mechanisms, demonstrating how XAI-driven analytics can uncover threshold effects that traditional linear models overlook. This research contributes to smart urban governance by positioning XAI as a bridge between big data analysis and age-sensitive urban decision-making, offering a framework to support behavior-responsive TOD and inclusive urban renewal.

Despite its contributions, several limitations remain. The analysis primarily focuses on macro- to meso-scale indicators for individuals aged 70, potentially overlooking micro-scale factors like street-level walkability and visual quality. Additionally, the unique policy context of Shanghai may limit direct generalization. Future research should prioritize quasi-experimental designs and multi-source spatiotemporal datasets to further unravel causal relationships and extend XAI into real-time, interactive planning platforms. Ultimately, by refining these AI-empowered frameworks, technological innovation can catalyze a transformation toward more human-centered, equitable, and resilient urban mobility ecosystems.

5. References

AFFAIRS, S. M. O. F. T. E. 2025. *Release of comprehensive statistical information on the elderly population, aging undertakings, and elderly care services in Shanghai in 2024* [Online]. Shanghai: Putuo District Government of Shanghai

CERIN, E., NATHAN, A., VAN CAUWENBERG, J., BARNETT, D. W. & BARNETT, A. 2017. The neighbourhood physical environment and active travel in older adults: a systematic review and meta-analysis. *International Journal of Behavioral Nutrition and Physical Activity,* 14.

DIAO, M., LIN, K. Y. & CHANG, Z. 2024. Impacts of new metro lines on the activity space of older people. *Transportation Research Part D-Transport and Environment,* 137.

EWING, R. & CERVERO, R. 2010. Travel and the Built Environment. *Journal of the American Planning Association,* 76**,** 265-294.

GEORGANOS, S., GRIPPA, T., GADIAGA, A. N., LINARD, C., LENNERT, M., VANHUYSSE, S., MBOGA, N., WOLFF, E. & KALOGIROU, S. 2021. Geographical random forests: a spatial extension of the random forest algorithm to address spatial heterogeneity in remote sensing and population modelling. *Geocarto International,* 36**,** 121-136.

GOVERNMENT, P. N. A. 2017. *Metro Lines in Shanghai* [Online]. Shanghai: Pudong New Area Government. Available: https://english.pudong.gov.cn/2017-07/19/c_84850_3.htm [Accessed].

GUO, C., JIANG, Y. Q., QIAO, R. L., ZHAO, J. B., WENG, J. C. & CHEN, Y. 2023. The nonlinear relationship between the active travel behavior of older adults and built environments: A comparison between an inner-city area and a suburban area. *Sustainable Cities and Society,* 99.

HAAN, C. 2024. *Free subway rides for seniors strains South Korea's railways, and ignites debate* [Online]. Koreapro. Available: https://koreapro.org/2024/05/free-subway-rides-for-seniors-strains-south-koreas-railways-and-ignites-debate/?utm_source=chatgpt.com [Accessed].

LIU, X., YU, Q., BIAN, W., YU, H., ZHANG, C., LIU, X., JIANG, H. & LUO, X. 2025a. Unraveling spatiotemporal dynamics of ridesharing potential: Nonlinear effects of the built environment. *Transportation Research Part D: Transport and Environment,* 139.

LIU, X. H., YE, Q., LI, Y., YANG, K. D. & SHAO, X. 2025b. Investigating relationships between ridesourcing and public transit using big data analysis and nonlinear machine learning: A case study of Shanghai, China. *Transportation Research Part a-Policy and Practice,* 192.

LUNDBERG, S. M. A. L., SU-IN. A Unified Approach to Interpreting Model Predictions. Advances in Neural Information Processing Systems (NeurIPS 2017), 2017. Curran Associates, Inc., 4765–4774.

WANG, Z. B., LI, S. H., LI, Y. J., LIU, D., LIU, S. Y. & CHEN, N. 2023. Investigating the Nonlinear Effect of Built Environment Factors on Metro Station-Level Ridership under Optimal Pedestrian Catchment Areas via the Machine Learning Method. *Applied Sciences-Basel,* 13.

WHO. 2024. *Ageing and health* [Online]. Geneva, Switzerland: World Health Organization. Available: https://www.who.int/news-room/fact-sheets/detail/ageing-and-health [Accessed 05.26 2025].

YANG, H. R., ZHANG, Q. R., WEN, J., SUN, X. & YANG, L. C. 2024a. Multi-group exploration of the built environment and metro ridership: Comparison of commuters, seniors and students. *Transport Policy,* 155**,** 189-207.

YANG, W., FEI, J., LI, Y. P., CHEN, H. & LIU, Y. 2024b. Unraveling nonlinear and interaction effects of multilevel built environment features on outdoor jogging with explainable machine learning. *Cities,* 147.

YANG, W., LI, Y., LIU, Y., FAN, P. & YUE, W. 2024c. Environmental factors for outdoor jogging in Beijing: Insights from using explainable spatial machine learning and massive trajectory data. *Landscape and Urban Planning,* 243.

ZANG, P., LU, Y., MA, J., XIE, B., WANG, R. Y. & LIU, Y. 2019. Disentangling residential self-selection from impacts of built environment characteristics on travel behaviors for older adults. *Social Science & Medicine,* 238.

ZOU, Q. R., YAO, X. M., ZHAO, P., WEI, H. & REN, H. 2018. Detecting home location and trip purposes for cardholders by mining smart card transaction data in Beijing subway. *Transportation,* 45**,** 919-944.